AIAA 93-0385
Control of Pressure Fluctuations in the Reattachment Region of a Supersonic Shear Layer

J. Poggie and A. J. Smits
Princeton University
Princeton, NJ

31st Aerospace Sciences Meeting & Exhibit
January 11-14, 1993 / Reno, NV

Control of Pressure Fluctuations in the Reattachment Region
of a Supersonic Free Shear Layer

J. Poggie* and A. J. Smits†

Princeton University, Princeton, NJ

January 31, 1993

Measurements of wall pressure fluctuations were made as part of an ongoing program to investigate the control of a turbulent, reattaching shear layer at Mach 2.9. The flow was disturbed near separation by air injection normal to the plane of the shear layer. This perturbation was found to dramatically increase the intensity of pressure fluctuations in the vicinity of reattachment. A local increase in shear layer growth rate was also observed in the perturbed flow.

Nomenclature

C_f	Skin Friction Coefficient
M	Mach number
p	Pressure
$\bar{p}$	Time-averaged pressure
p'	Fluctuating pressure $(p - \bar{p})$
p_t	Stagnation pressure
x	Distance along the ramp face
Re_θ	Momentum thickness Reynolds Number
U	Speed
Π	Turbulent boundary layer wake strength parameter
δ	Boundary layer or shear layer thickness
ρ	Density

Introduction

Intense pressure fluctuations, especially in conjunction with high temperature, are known to greatly increase the probability of fatigue failure. These factors are especially severe in the vicinity of reattachment in a separated supersonic flow. Such flows occur in a variety of applications; one example is a deflected control surface on a high-speed aircraft. A greater understanding of the physics of this class of flow would help in efforts to alleviate fatigue failure problems.

In a recent paper, Poggie and Smits [1] showed that the structure of a supersonic reattaching shear layer could be altered through air injection near the separation point. In particular, a remarkable increase in the unsteadiness of the reattachment shock system was observed when the air injection was localized near the centerline of the experimental model. In the present work, this phenomenon was examined in more detail by measuring wall pressure fluctuations in the vicinity of reattachment.

The experimental model (figure 1) was designed by Baca [2] so that a Mach 2.9 turbulent boundary layer separates at a backward-facing step with no change in flow direction. The resulting shear layer reattaches on a 20° ramp, passing through an oblique shock system, and develops into an equilibrium turbulent boundary layer.

The undisturbed flowfield for this particular experimental model has been investigated in several previous studies. The mean flowfield was surveyed by Settles et al. [3]. Horstman et al. [4] conducted a numerical simulation of the flow using a turbulence model, and compared the results with the experimental data. Hayakawa et al. [5] made hotwire surveys, and Shen et al. [6] measured wall pressure fluctuations. A detailed description of the flow can be found in Poggie and Smits [1].

Experimental Procedure

The experiments were conducted in the first test section of the Princeton University 203 mm by 203 mm high Reynolds number blowdown wind tunnel. This facility, previously described by Vas and Bogdonoff [7], can operate with stagnation pressures ranging from about 400 kPa to over 1400 kPa, and at Mach numbers from two to four. In this study, the stagnation pressure and freestream Mach number were 690 kPa ±1% and 2.94 ±0.01, respectively. In a typical run, the

---

* Graduate Student, member AIAA
† Professor, member AIAA

stagnation temperature was initially 270 K and dropped by about 4% over one minute. The tests were made under near adiabatic wall conditions, and with a freestream turbulence intensity of 0.0075 [5].

The experimental model is shown in figure 1. It consists of a wedge-shaped plate containing a cavity 25.4 mm deep, starting 229 mm downstream of the leading edge. A 20° ramp, 160 mm long, lies 61.9 mm downstream of the start of the cavity. When the plate is installed parallel to the freestream flow in the wind tunnel, the roof of the tunnel is 152.4 mm above the plate, and the plate spans the 203 mm width of the test section. In order to avoid interference with the side wall boundary layers, the cavity and ramp are inset by 25.4 mm on each side of the test section, and aerodynamic fences are attached to the sides of the ramp.

The inlet boundary condition to the cavity flowfield was provided by the boundary layer that formed on the upstream part of the model. It was surveyed by Baca [2] at a location 25.4 mm upstream of the backward-facing step. He found that it was a near-equilibrium turbulent boundary layer, with $Re_\theta = 10100$, $\delta = 2.9$mm, $C_f = 0.00144$, and $\Pi = 0.73$.

As described in Poggie and Smits [1], flow control was effected through air injection near the backward-facing step in the experimental model. The model was modified to include two spanwise rows of holes, one 12.7 mm upstream of the step, and the other 12.7 mm downstream of the step. Each row was 101.6 mm long, and consisted of 33, 1.6 mm diameter holes (see figure 1c).

Two techniques of flow visualization were used. Schlieren photographs were made using a Z-type schlieren system. The mirrors in this system are 304.8 mm in diameter, and have a focal length of 2.54 m. A strobe lamp provided a flash less than 2 microseconds in duration at a repetition rate of 30 Hz. The images were recorded by a CCD camera on 0.5 in VHS video tape.

Images of the flow were also made through Rayleigh scattering of ultraviolet (UV) light. Illumination was provided by a Quantel International YG661 laser. The output of the laser was frequency-doubled to a wavelength of 266 nm, focused in one plane with a converging lens, and spread out in the perpendicular plane using a diverging lens, thus forming a trapezoidal sheet. This sheet was passed through UV-transparent quartz windows in the wind tunnel. A high sensitivity IIT CID camera recorded the scattered ultraviolet light through another quartz window.

The duration of the laser pulse was about 4 ns, and the thickness of the sheet of laser light was less than 0.2 mm. The UV camera had 180 lines of resolution, and the data were recorded at a rate of 10 Hz.

The scattering particles were ice clusters on the order of 10 nm in diameter (Wegener and Stein [8]) that form naturally in flow. Qualitatively, it has been observed that the ice cluster density is nearly proportional to the local air density, except when the temperature rises to a level where the ice clusters vaporize. High temperature regions therefore appear dark, as the scattering cross-section of the ice clusters is much greater than that of air.

It was necessary to modify the model for the flow visualization experiments in order to obtain optical access to the full shear layer. The aerodynamic fences were removed, and the height of the cavity sidewalls was reduced by 9.5 mm. Under these conditions, a weak expansion fan exists at the lip of the cavity. The ratio of the upstream pressure to the cavity pressure was 1.01 with the fences and sidewall inserts in place, and was 1.04 with them removed. Mean pressure measurements on the 20° ramp (discussed below) indicate that the behavior of the flow is not significantly different with the fences and inserts removed.

Measurements were made of both mean and fluctuating pressure along the centerline of the 20° ramp. Mean pressure measurements were made using a scanivalve system, in which an automatic valve allowed a single pressure transducer to read pressures from a set of 57 taps in the experimental model. A one second delay was imposed between readings to allow the system to respond to each new pressure.

The pressure fluctuations were measured with miniature differential pressure transducers manufactured by Kulite Semiconductor Products. Each transducer has a 0.71 mm silicon diaphragm on which a fully active Wheatstone bridge is bonded atomically. Previous experiments (Spina [9]), as well as data provided by the manufacturer, have shown that these transducers have a flat frequency response up to about 80-100 kHz.

The Kulite pressure transducers were calibrated statically at the operating temperature. Checks made before and after wind tunnel runs showed that the calibration was consistently linear and repeatable. Shock tube tests by Raman [10] have shown that static calibrations of transducers of this type differ by only a few percent from dynamic calibrations. Signals from the transducers were amplified, band-pass filtered between 10 Hz and 100 kHz, and sampled digitally at a rate of 250 kHz by a crate-based CAMAC data acquisition system. Data were obtained simultaneously for four channels in files of four records, each containing 16384

contiguous points per record.

Results

In recent work (Poggie and Smits [1]), it was found that air injection uniformly distributed across the span of the experimental model merely shifted the shear layer up due to increased pressure in the cavity, while localized air injection caused a dramatic change in the flow. Thus, the disturbance in the current experiment was generated by injecting air through the three holes nearest to the centerline in the cavity of the experimental model (figure 1c). Air was supplied from a storage tank maintained at 609 kPa ±1% and 295 K ±1%. The mass flux (ρU) through the three holes was on the order of $30 \, kg/m^2/s$, and the ratio of the mass flux through the holes to the freestream mass flux was on the order of 0.1.

Schlieren photographs were made of the flow to qualitatively assess the effects of air injection. Figures 3 and 4 show schlieren photographs of two views of the model. The knife edge was horizontal, and the freestream flow was from left to right. The field of view is about 110 mm by 80 mm in both sets of images, and the orientation of the views is sketched in figure 2. Note that part of the cavity region is obscured by the sidewalls of the model.

Figure 3a shows a side view of the undisturbed flow in the vicinity of separation. An expansion fan is visible, centered at the backward-facing step. (Schlieren photographs of the flow with the sidewall inserts and the aerodynamic fences in show a much smaller expansion fan, but reveal little detail of the rest of the flow.) The weak wave upstream of the step is probably caused by the upstream row of air holes. The upper and lower edges of the developing shear layer are clearly visible, and waves appear to be emanating from the upper edge.

The corresponding view in the vicinity of reattachment is show in figure 4a. The shear layer and expansion fan are visible as in the upstream view. The shear layer can be seen to reattach onto the 20° ramp, passing through a system of shocks and compression waves, and to redevelop into a new boundary layer.

Figure 3b shows the effect of injecting air into the flow near separation. The shear layer appears to have thickened and shifted down (note the increased size of the expansion fan). This behavior suggests that entrainment has increased in the shear layer to balance the mass flow into the cavity region from the jet of injected air. The edges of the shear layer appear to be more convoluted in the perturbed flow, and increased activity is present in the waves above the shear layer and in the recirculating flow below it.

A more dramatic effect of the localized air injection can be seen in the view of the reattachment region of the flow in figure 4b. The reattachment shock system is greatly distorted. The large oblique shock seems to have split in two in this image, with one part greatly curved. Examination of multiple schlieren images shows that the unsteadiness of the shock system is greatly increased in the disturbed flow.

In addition, the boundary layer on the ramp appears to have thickened in the disturbed flow. Close inspection of the schlieren photograph also reveals a region in the redeveloping boundary layer where the sign of the density gradient may be reversed.

In order to further investigate the three dimensional nature of the disturbed flow field, the Rayleigh scattering method was utilized to visualize the effects of a slightly different configuration of air injection. A laser sheet was passed through the side walls of the tunnel, about 32 mm from the backward-facing step, and was viewed from above. The laser sheet was rotated so that its normal made a 45° angle with the freestream flow (figure 5a). The images were stretched linearly in order to correct for the foreshortening introduced by this viewing angle.

The results are shown in figure 5. The center of each image is about 32 mm from the tunnel centerline and 32 mm downstream of the backward-facing step. Each image is lined up with a group of five holes that were supplied with a stagnation pressure of 1.0 MPa. The shear layer thickness at this location, marked δ, is about 7mm. Three cases are shown: the undisturbed flow, air injection from the upstream row of holes, and air injection from the downstream row of holes. Air injection creates a bulge in the shear layer with a width on the order of the shear layer thickness. The bulge is smaller in the images with blowing downstream of the step -- possibly because the disturbance spread less in the shorter distance between the location of air injection and the plane of the laser sheet. The shock induced by the jets of injected air is also faintly visible in the images. The results indicate that the increase in shear layer growth rate is localized in its spanwise extent.

In the case of air injection through three holes, measurements were made of the mean and fluctuating pressure along the centerline of the ramp. Figure 6a compares measurements of the mean pressure in the undisturbed flow with the results of Baca [2]. The pressure distributions match closely. The pressure rises monotonically from the level of the upstream boundary layer to the level predicted by oblique shock theory for a Mach number of 2.9 and a 20° turning angle

(indicated by the horizontal line in the figure).

Figure 6b compares the mean pressure distribution in the undisturbed flow to the distribution with air injection. In the disturbed flow, the pressure rise begins sooner, but the pressure increases more slowly with streamwise distance, and reaches the same level downstream. The longer region of changing pressure may indicate a wider range of shock motion.

Figure 6c shows the mean pressure distribution with the aerodynamic fences and sidewall inserts removed. The effect of air injection is seen to be qualitatively the same as the case with the fences and inserts in, but somewhat greater in magnitude. Thus the flow visualization data taken under these conditions should show, qualitatively, the same phenomena as the other data.

Figure 7 shows the ratio of the r.m.s. fluctuating pressure to the mean pressure along the ramp. Air injection causes a significant increase in the intensity of the pressure fluctuations, probably due to increased unsteadiness in the reattachment shock system. Figure 8 shows that the results for the undisturbed case agree with the data of Shen et al. [6] within the experimental uncertainty.

Conclusions and Future Work

Air injection appeared to cause a local increase in the shear layer growth rate when the spanwise extent of the jet was on the order of the shear layer thickness. The downstream effect was increased unsteadiness of the reattachment shock system, accompanied by an increase in the intensity of wall pressure fluctuations. Thus, strong three dimensional perturbations should be minimized in applications where fatigue failure could be a problem. Future experiments will investigate the spanwise extent of the effect of air injection on the flow near reattachment.

The present experimental program has artificially created shock unsteadiness with three dimensional perturbations. It would therefore be reasonable to investigate in future work whether naturally occurring disturbances of a similar type might contribute significantly to shock unsteadiness.

References

1. Poggie, J., and Smits, A. J., "The Dynamics and Control of Fluctuating Pressure Loads in the Reattachment Region of a Supersonic Free Shear Layer," AIAA Paper 92-0178 (1992).

2. Baca, B. K., "An Experimental Study of the Reattachment of a Free Shear Layer in Compressible Turbulent Flow," M.S.E. Thesis, Princeton University, Princeton, NJ (1981).

3. Settles, G. S., Baca, B. K., Williams, D. R., and Bogdonoff, S. M., "Reattachment of a Compressible Turbulent Free Shear Layer," AIAA J., vol. 20, p. 60 (1982).

4. Horstman, C. C., Settles, G. S., Williams, D. R., and Bogdonoff, S. M., "A Reattaching Free Shear Layer in Compressible Turbulent Flow," AIAA J., vol. 20, p. 60 (1982).

5. Hayakawa, K., Smits, A. J., and Bogdonoff, S. M., "Turbulence Measurements in a Compressible Reattaching Shear Layer," AIAA J., vol. 20, p. 79 (1982).

6. Shen, Z.-H., Smith D. R., and Smits, A. J., "Wall Pressure Measurements in the Reattachment Region of a Supersonic Free Shear Layer," AIAA Paper 90-1461 (1990).

7. Vas, I. E., and Bogdonoff, S. M., "A Preliminary Report on the Princeton University High Reynolds Number 8 in x 8 in Supersonic Tunnel," Internal Memorandum No. 39, Gas Dynamics Laboratory, Princeton University, Princeton, NJ (1971).

8. Wegener, P. P., and Stein, G. D., "Light-Scattering Experiments and Theory of Homogeneous Nucleation in Condensing Supersonic Flow," 12th International Symposium on Combustion, p. 1183 (1968).

9. Spina, E. F., "Organized Structures in a Supersonic Turbulent Boundary Layer," Ph. D. Thesis, Princeton University, Princeton, NJ (1988).

10. Raman, K. R., "A Study of Surface Pressure Fluctuations in Hypersonic Turbulent Boundary Layers," NASA CR-2386 (1974).

(a)

(b)

(c)

Figure 1: (a) Diagram of flowfield. After Baca
[2]. (b) Experimental model. After Baca [2]. (c)
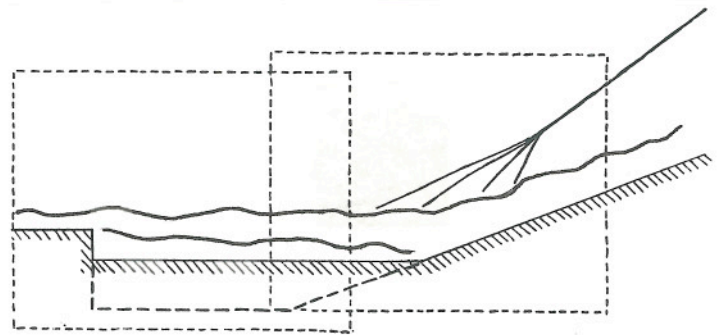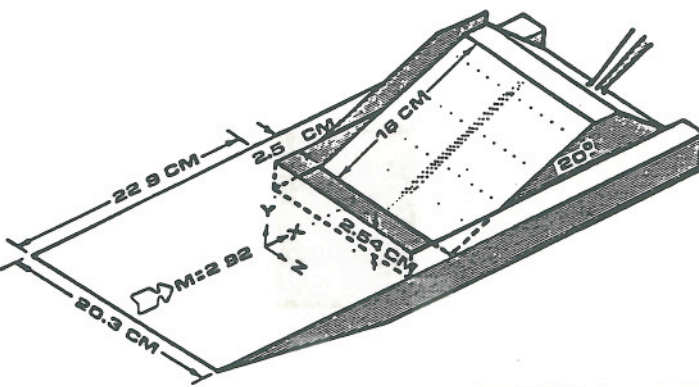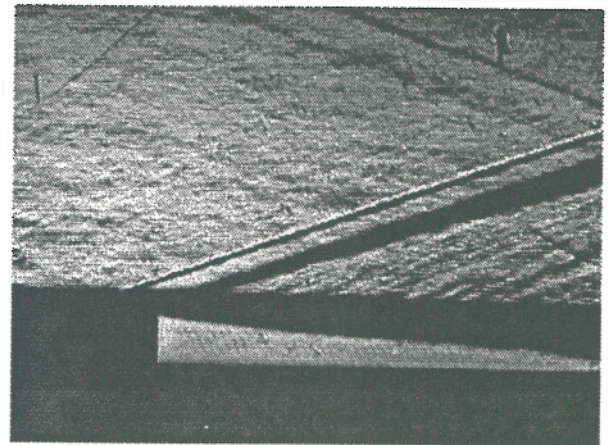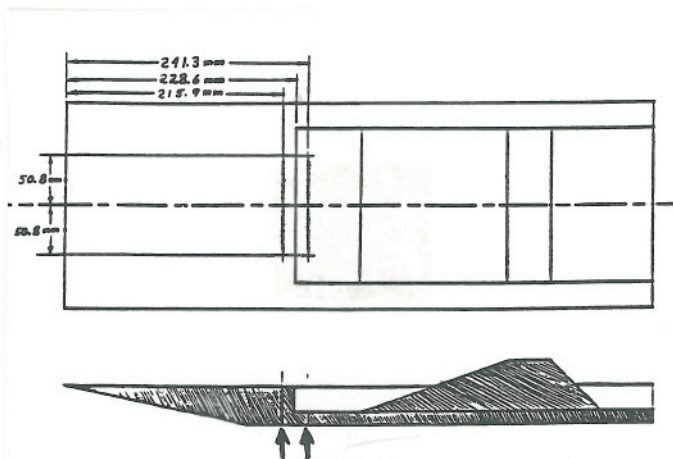Holes added to model for air injection.
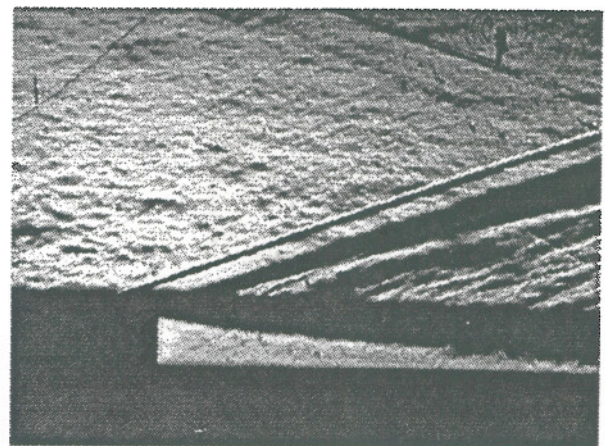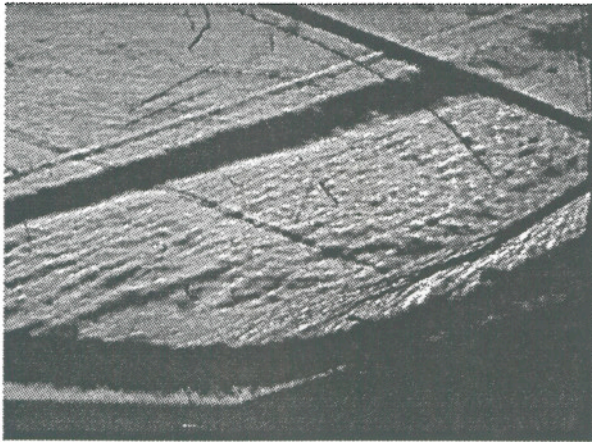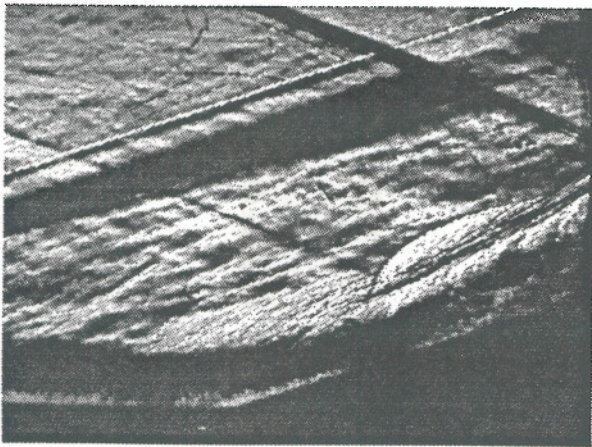

Figure 2: Field of view in schlieren photographs.

(a)

(b)

Figure 3: Schlieren photographs in the vicinity of
separation. (a) Undisturbed flow. (b) Perturbed
flow.

(a)

(a)

(b)

(b)

Figure 4: Schlieren photographs in the vicinity of reattachment. (a) Undisturbed flow. (b) Perturbed flow.
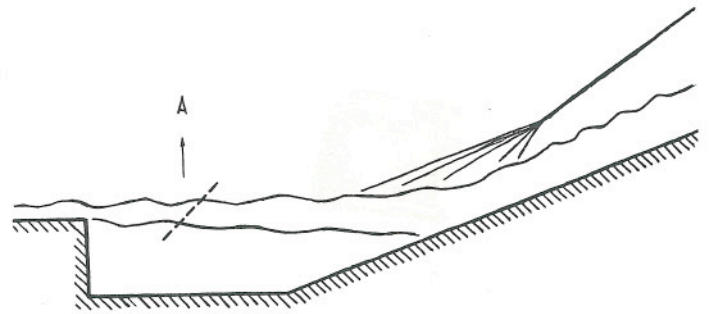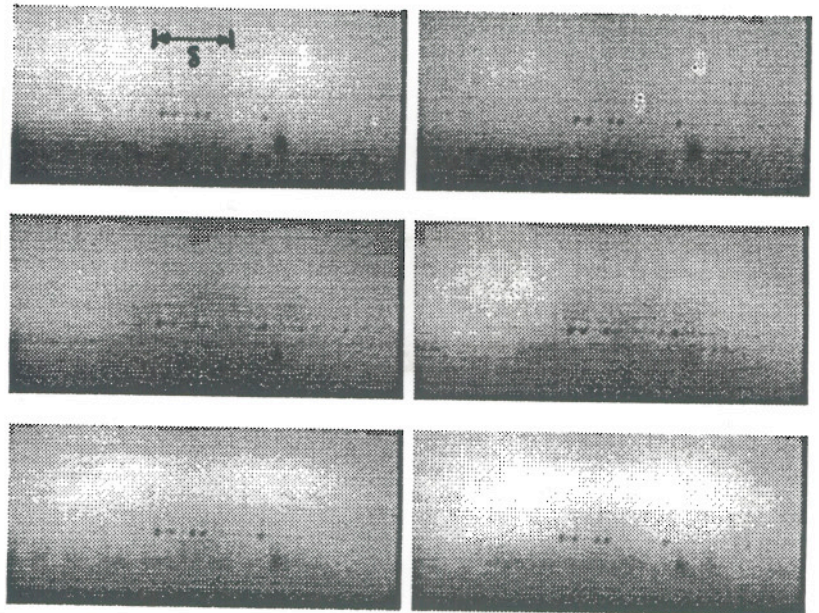
Figure 5: (a) Orientation of laser sheet. (b) Rayleigh scattering images. Top: undisturbed flow. Middle: air injection upstream of the step. Bottom: air injection downstream of the step.
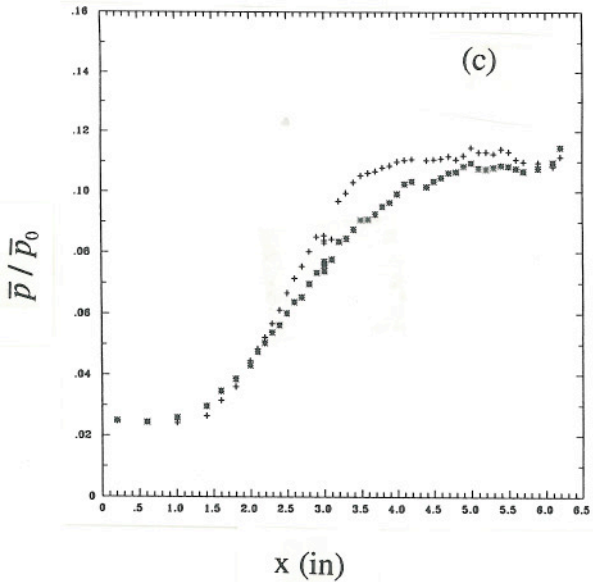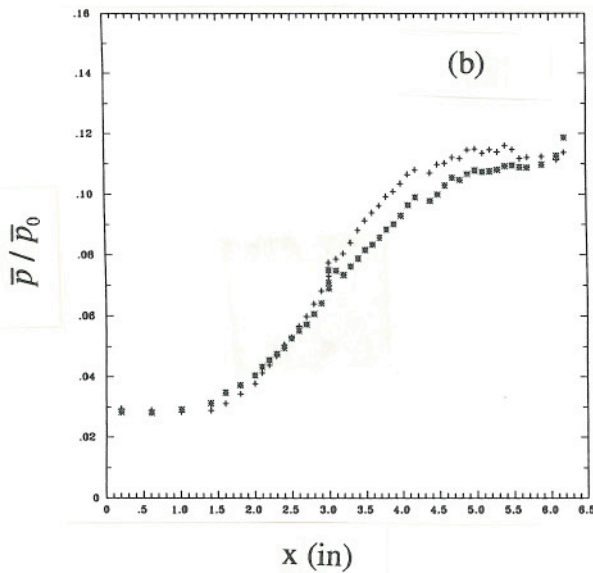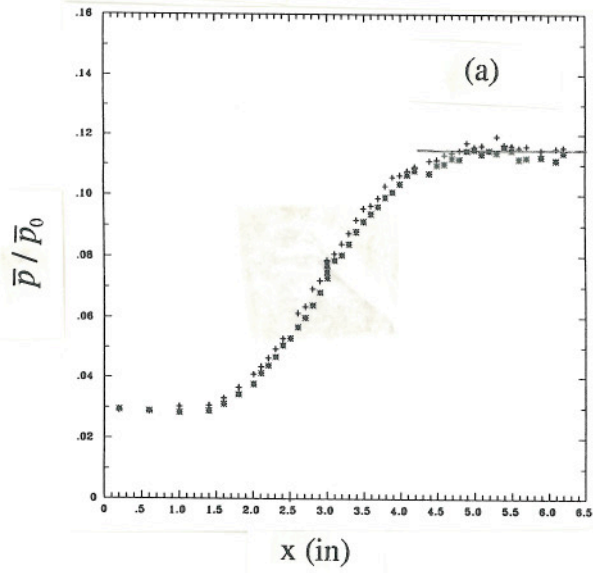
Figure 6: Mean pressure along the ramp face. (a) Undisturbed Flow: * - current study, + - Baca [2]. (b) Effect of flow perturbation: + - undisturbed case, * - air injection. (c) Aerodynamic fences and sidewall inserts removed: + - undisturbed flow, * - air injection.
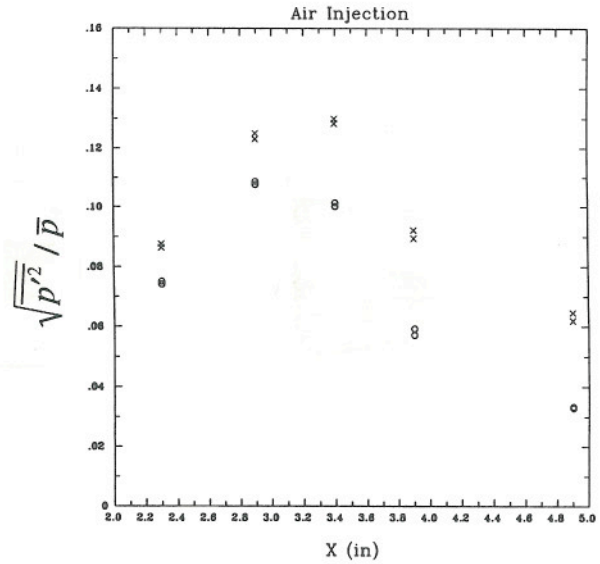
Figure 7: RMS. fluctuating pressure along the ramp face. O - undisturbed flow, X - air injection.
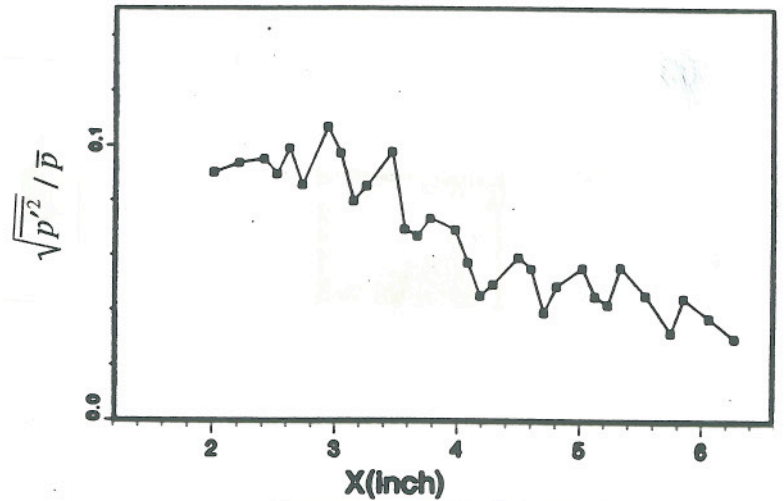
Figure 8: RMS fluctuating pressure along the ramp face in the undisturbed flow. After Shen et al. [6].